# Hydriding Properties of $MgH_2$-$Mg_2Ni_{0.8}Co_{0.2}$ Composites Obtained by Ball Milling

Tsveta Mandzhukova[a], Jean-Louis Bobet[b], Maria Khrussanova[a], and Pavel Peshev[a]

[a] Institute of General and Inorganic Chemistry, Bulgarian Academy of Sciences, Acad. G. Bonchev Str., Building 11, 1113 Sofia, Bulgaria
[b] Institut de Chimie de la Matière Condensée de Bordeaux (ICMCB), CNRS, (UPR 9048), Université Bordeaux 1, 87 Avenue du Docteur A. Schweitzer, 33608 Pessac Cedex, France

Reprint requests to Ts. Mandzhukova. Fax: +359 2 8705024. E-mail: tsvetam@svr.igic.bas.bg

*Z. Naturforsch.* **2007**, *62b,* 915 – 921; received April 3, 2007

*Dedicated to Dr. Bernard Chevalier on the occasion of his 60th birthday*

The hydrogen absorption-desorption characteristics of composites consisting of 90 wt. % $MgH_2$-10 wt. % $Mg_2Ni_{0.8}Co_{0.2}$ prepared by ball milling for 30 and 180 min under argon have been investigated. The results obtained have been compared with those for the 90 wt. % Mg-10 wt. % $Mg_2Ni_{0.8}Co_{0.2}$ composite synthesized in the same medium after 30 min of milling. The presence of the $Mg_2Ni_{0.8}Co_{0.2}$ phase has been found to improve the hydriding kinetics of magnesium, the absorption capacity remaining high at temperatures below 573 K. The use of magnesium hydride instead of magnesium has proved to have a favorable effect on the properties of the composites after prolonged activation in an inert medium. It has been established that the absorption-desorption characteristics of the composite 90 wt. % $MgH_2$-10 wt. % $Mg_2Ni_{0.8}Co_{0.2}$ activated mechanically for 180 min are comparable with those of the composite 90 wt. % Mg-10 wt. % $Mg_2Ni_{0.8}Co_{0.2}$ after mechanical activation for only 30 min. The favorable absorption-desorption characteristics of the composites have been explained with the catalytic effect of the additive, the presence of magnesium hydride and the duration of ball milling.

*Key words:* Hydrogen Storage, Magnesium Composites, Ball Milling, Intermetallic Additives

## Introduction

Among the hydrogen storage systems, those based on magnesium are of particular interest because magnesium has a high absorption capacity and a low price. However, a serious obstacle to the application of these systems are the poor hydriding-dehydriding kinetics and the high temperatures and pressures at which reversible hydrogen absorption proceeds. To find a practical application, such materials should (i) have a high absorption capacity and good hydriding-dehydriding kinetics, (ii) permit proceeding of hydrogen absorption-desorption processes under conditions milder than those of pure magnesium, and (iii) be suitable for cycling without a drastic decrease in absorption capacity. A way of eliminating these disadvantages with respect to magnesium is the application of the mechanical activation method [1 – 5]. The nanocrystals or amorphous materials obtained by this method have improved the hydrogen sorption characteristics, which is explained by the presence of defects and dislocations playing the role of nucleation sites of the hydride phase while the interface boundaries facilitate the diffusion of hydrogen to and from the matrix. During mechanical activation in inert or hydrogen medium, the partially formed oxide layer is destroyed and the surface accessible to reaction is increased. Simultaneously, due to the fact that the magnesium particles tend to stick together, agglomerates are formed. One of the ways to overcome this problem is to use the more brittle magnesium hydride which yields, after mechanical activation, finely disperse composites [3 – 5]. On the other hand, the use of various additives (metals, non-metals, metal oxides or intermetallics) proved very advantageous for improving the absorption-desorption characteristics of such mechanically alloyed magnesium composites [6 – 14]. Previous studies [14] showed the positive effect of the presence of an intermetallic compound of the type $Mg_2Ni_{1-x}T_x$ ($T$ = Fe, Co) on the hydriding-dehydriding kinetics and the absorption capacity of magnesium in mechanically alloyed magnesium composites. It has been es-

tablished that the simultaneous presence in the intermetallic compound $Mg_2Ni_{1-x}Co_x$ of the two transition metals, nickel and cobalt, has a very favorable effect on both the hydriding kinetics and the absorption capacity of the magnesium composites.

Taking into account literature data on the positive effect of magnesium hydride and of the simultaneous presence of cobalt and nickel in the additive to magnesium composites obtained by mechanical activation, we carried out the present investigation on the hydrogen absorption-desorption properties of the composites 90 wt. % $MgH_2$-10 wt. % $Mg_2Ni_{0.8}Co_{0.2}$ obtained after different ball milling times. In order to prove the role of magnesium hydride, the experimental results obtained were compared with those of an investigation on a material with a similar composition (90 wt. % Mg-10 wt. % $Mg_2Ni_{0.8}Co_{0.2}$) but containing pure magnesium instead of $MgH_2$.

## Experimental Section

The magnesium hydride used was synthesized by hydriding powdery magnesium (99.9 % purity) at $T$ = 593 K and $P$ = 5 MPa for 96 h. The intermetallic compound $Mg_2Ni_{0.8}Co_{0.2}$ was prepared using Mg, Ni and Co powders of 99.9 % purity, the Mg/Ni+Co ratio being 2.05 : 1. The homogenized mixture was pelletized and heated at 823 K for 120 h under argon.

The composites 90 wt. % $MgH_2$-10 wt. % $Mg_2Ni_{0.8}Co_{0.2}$ were obtained by mechanical alloying in a Fritsch Pulverisette 5 planetary ball mill under argon with milling durations of 30 and 180 min using stainless-steel balls. The ball-to-sample weight ratio was 10 : 1 and the rotation speed 200 rpm. The composite 90 wt. % Mg-10 wt. % $Mg_2Ni_{0.8}Co_{0.2}$ was prepared under the same conditions and mechanically activated for 30 min. Further on in this article, these composites will be denoted as follows:

Composite A: 90 wt. % $MgH_2$-10 wt. % $Mg_2Ni_{0.8}Co_{0.2}$, ball-milled for 30 min; composite B: 90 wt. % $MgH_2$-10 wt. % $Mg_2Ni_{0.8}Co_{0.2}$, ball-milled for 180 min; composite C: 90 wt. % Mg-10 wt. % $Mg_2Ni_{0.8}Co_{0.2}$, ball-milled for 30 min.

The phase composition of the synthesized compounds $MgH_2$ and $Mg_2Ni_{0.8}Co_{0.2}$, as well as of the initial, hydrided and dehydrided composites, was controlled by X-ray phase analysis using Cu$K_\alpha$ radiation. In order to check the morphology and homogeneity of the composites and the intermetallic compound, scanning electron microscopy was applied as well as electron microprobe analysis with a CAMECA SX-100 instrument. Particle size distribution of the composites was checked using a Malvern 2000 device.

The absorption-desorption properties of the composites were determined by the volumetric method described in [15]. Hydrogen absorption by the composites obtained was investigated at temperatures of 373, 423, 473, 523, and 573 K and a pressure of 1 MPa, while desorption was studied at $T$ = 553 K, 573 K and 603 K and $P$ = 0.02 MPa. The desorption properties at 573 K were also determined at a pressure of 0.15 MPa.

## Results and Discussion

X-Ray phase analysis has shown, along with the main $Mg_2Ni$-type phase, a negligible amount of $MgNi_2$ and traces of Co and Ni in the synthesized intermetallic compound. Fig. 1 presents the X-ray patterns of the initial composites A and B while Fig. 2 shows those of the dehydrided ones. It is evident that the initial composite B, which has been activated for a longer

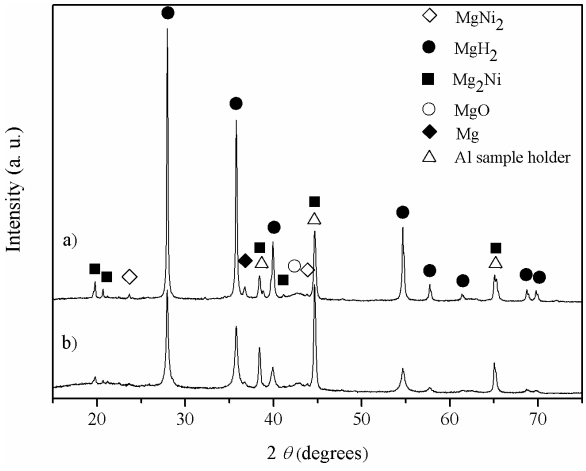


Fig. 1. X-Ray patterns of the initial composites A (a) and B (b).

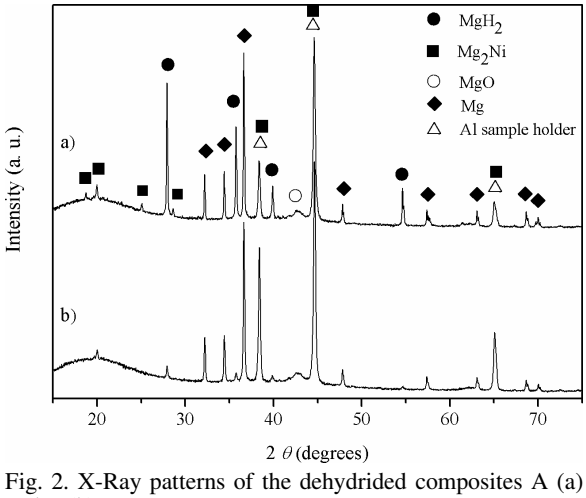


Fig. 2. X-Ray patterns of the dehydrided composites A (a) and B (b).

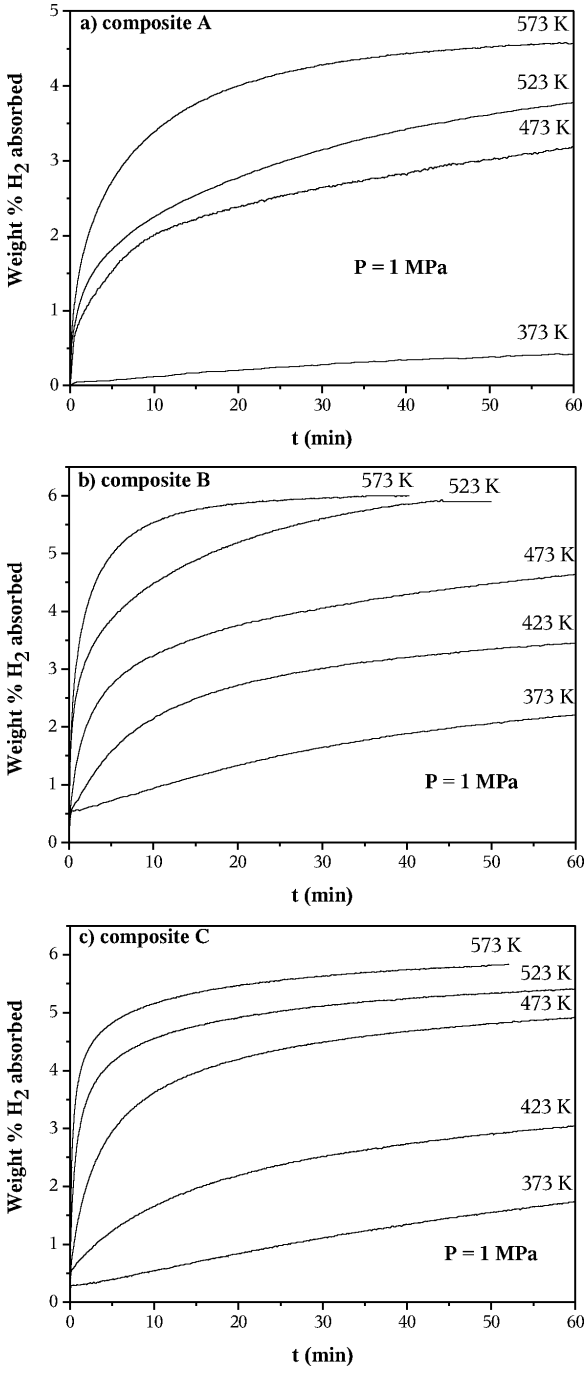


Fig. 3. Curves of the hydrogen absorption kinetics of the composites at different temperatures and a pressure of 1 MPa: (a) composite A; (b) composite B; (c) composite C.

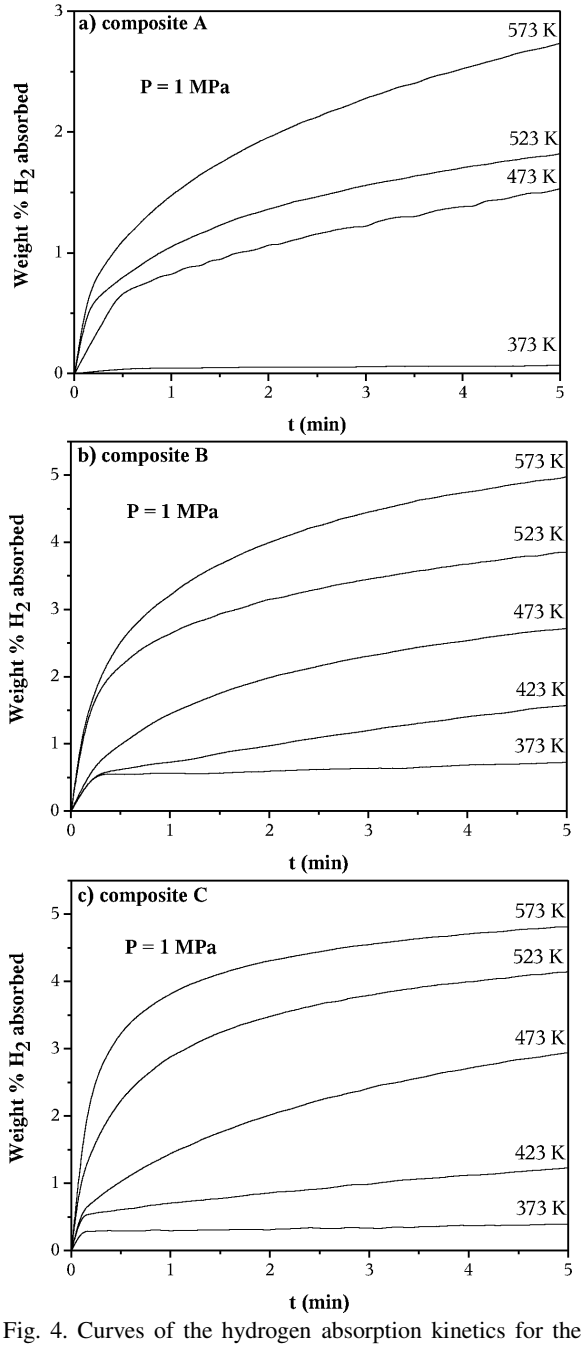


Fig. 4. Curves of the hydrogen absorption kinetics for the first 5 min of hydriding of: (a) composite A; (b) composite B; (c) composite C.

time, has a more pronounced tendency to amorphization.

Fig. 3 illustrates the curves of the hydriding kinetics of the three composites investigated at different temperatures and a pressure of 1 MPa. It is obvious that the absorption capacities attained are high and remain rel-

| Sample | 573 K | | 523 K | | 473 K | | 423 K | | 373 K | |
|---|---|---|---|---|---|---|---|---|---|---|
| | 10 min | 40 min | 10 min | 40 min | 10 min | 40 min | 10 min | 40 min | 10 min | 40 min |
| A | 3.39 | 4.44 | 2.3 | 3.42 | 2.01 | 2.81 | – | – | 0.12 | 0.34 |
| B | 5.54 | 6 | 4.49 | 5.87 | 3.22 | 4.29 | 2.13 | 3.2 | 0.94 | 1.88 |
| C | 5.16 | 5.74 | 4.55 | 5.24 | 3.63 | 4.67 | 1.65 | 2.74 | 0.55 | 1.35 |

Table 1. Absorption capacity values (wt. %) of the composites at different temperatures and hydriding durations of 10 and 40 min.

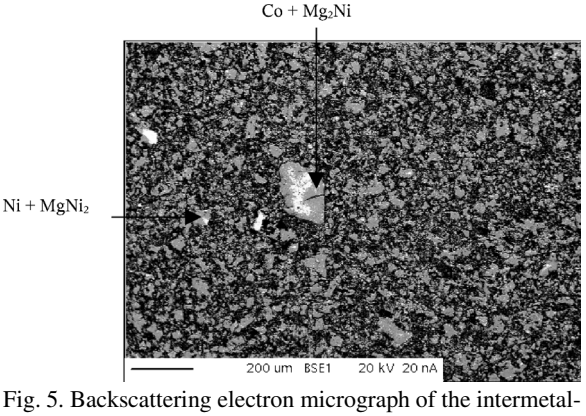


Fig. 5. Backscattering electron micrograph of the intermetallic compound $Mg_2Ni_{0.8}Co_{0.2}$.

atively high when the temperature drops to 373 K. Table 1 shows the absorption capacity values of the composites reached after 10 and 40 min of hydriding at the corresponding temperatures and a pressure of 1 MPa. Comparison of the experimental data on composites B and C shows the highest capacity values for composite B. As to the hydriding kinetics, with composite C these are better at 573 K. This can be established from the shape of the absorption curves for the three composites during the first 5 min of the reaction (Fig. 4). The experimental data also show that the very good properties of composite B are comparable with those of composite C obtained on the basis of pure magnesium. These two composites reach more than 90 – 92 % of their absorption capacity already during the first 10 min of hydriding, *i. e.* 72 – 77 % of the theoretical capacity which, for these systems, is 7.2 wt. %.

The results obtained illustrate the catalytic effect of the added intermetallic $Mg_2Ni_{0.8}Co_{0.2}$. The presence of this intermetallic compound is associated with the formation of a second hydride, $Mg_2NiH_4$, which, on its part, increases the interface and facilitates the nucleation. The presence of the $MgNi_2$ phase, which is not hydrided, facilitates the diffusion of hydrogen along the boundaries of the $MgNi_2$ grains, simultaneously enhancing its diffusion into the $Mg_2Ni$ particles. On the other hand, the presence on the surface of Ni and Co clusters which play the role of active sites during dissociative hydrogen chemisorption, also facilitates

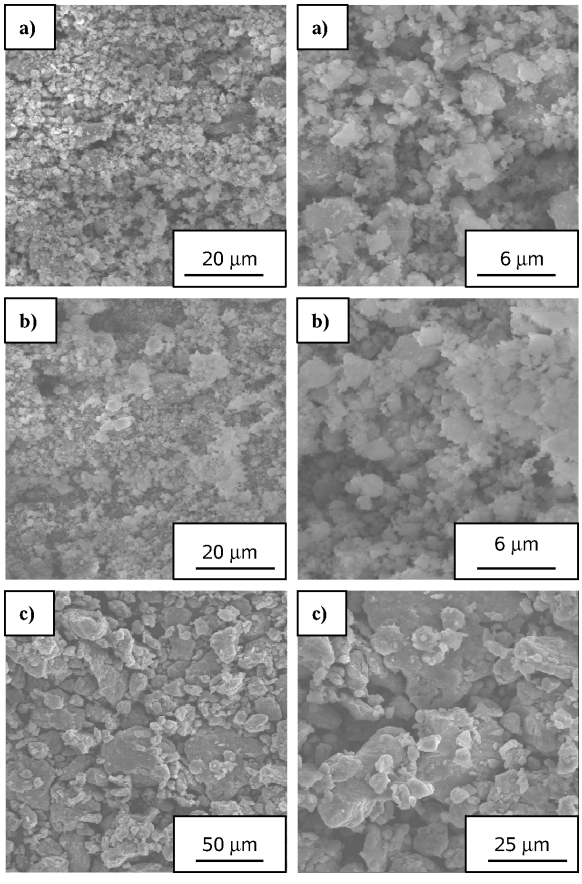


Fig. 6. SEM microphotographs of the three initial composites (a) composite A; (b) composite B; (c) composite C.

the hydriding of magnesium. The presence of metallic cobalt and nickel on the surface is evidenced by the electron microphotograph shown in Fig. 5. An additional factor in creating a more reactive composite surface is the mechanical activation in an inert medium. The resulting composites have different dispersities depending on the main component and the milling time.

This is also evidenced by the SEM microphotographs of the three composites (Fig. 6), which show that composite B subjected to a prolonged milling has a smaller particle size than composite A, while sample C shows small size particles surrounded by larger agglomerates.

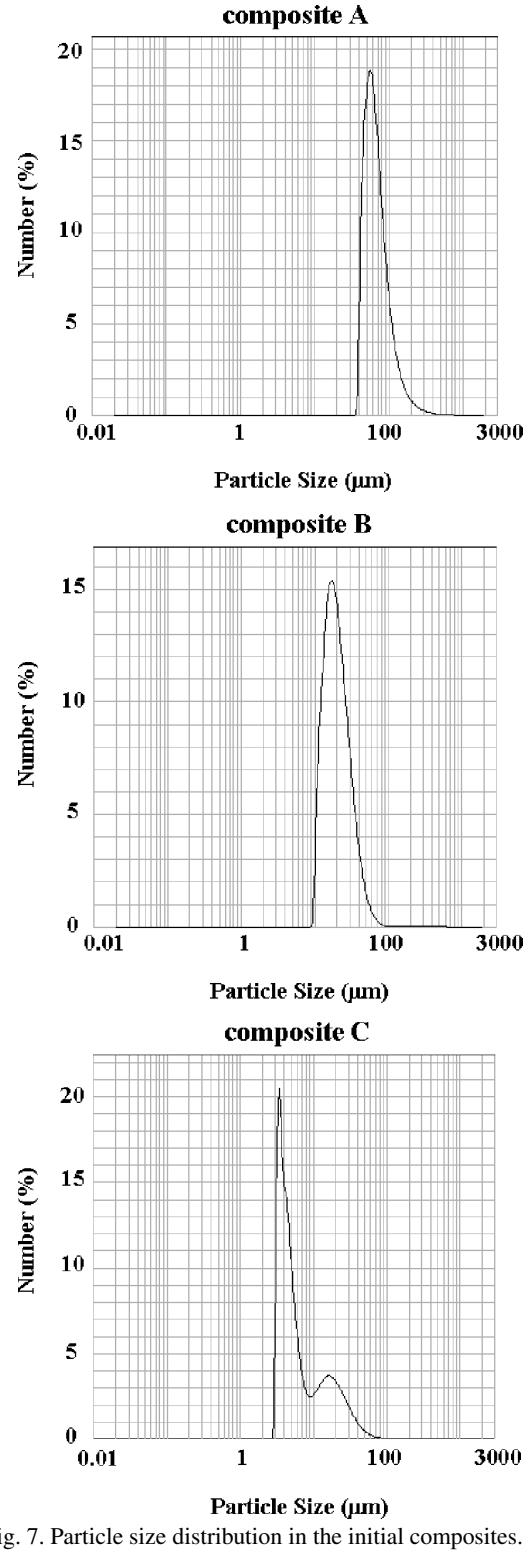


Fig. 7. Particle size distribution in the initial composites.

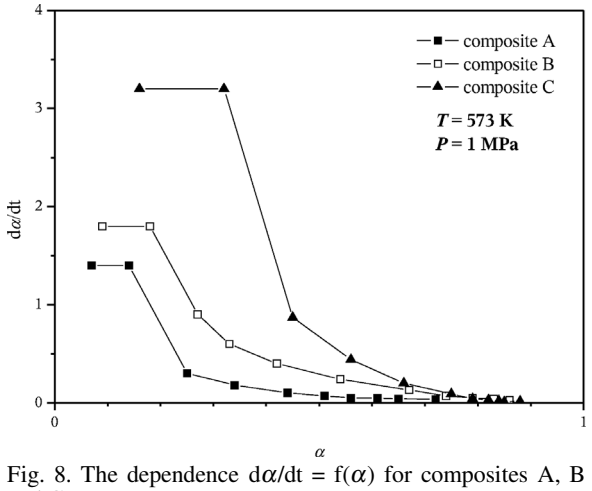


Fig. 8. The dependence $d\alpha/dt = f(\alpha)$ for composites A, B and C.

The data on particle size distribution of the composites obtained by laser granulometry measurements confirm the SEM results. As shown in Fig. 7 the two composites containing magnesium hydride (A and B) are monodisperse and have particle sizes of 50 $\mu$m (A) and 20 $\mu$m (B), respectively, which also improves the absorption characteristics of the composite activated for a longer time. Sample C shows a bimodal particle size distribution of about 4 $\mu$m (prevailing) and of about 15 $\mu$m. The enhanced dispersion of this component is probably the reason for its good hydriding kinetics.

The experimental values of the time needed for absorption of 20 – 80 % of the maximum hydrogen uptake can be used to calculate the mean hydrogen absorption rate as proposed by Dehouche *et al.* [16]. The calculated hydriding rates at $T$ = 573 K are 0.20 % $H_2$ $min^{-1}$ for composite A, 0.90 % $H_2$ $min^{-1}$ for B and 1.06 % $H_2$ $min^{-1}$ for C. The more unfavorable absorption properties of composite A are ascribed to the fact that a smaller amount of magnesium participates in the hydriding process because part of the magnesium hydride remains undecomposed after the desorption process. This is evidenced by the X-ray patterns of the dehydrided composites (Fig. 2). On the other hand, the better absorption properties of composite B are a result of prolonged mechanical activation. This is a fact described in the literature on magnesium composites obtained with the participation of magnesium hydride [9 – 13, 17 – 19].

The behaviour of the three composites may be explained on the basis of the change in the rate controlling step of the hydriding reaction. The shape of the

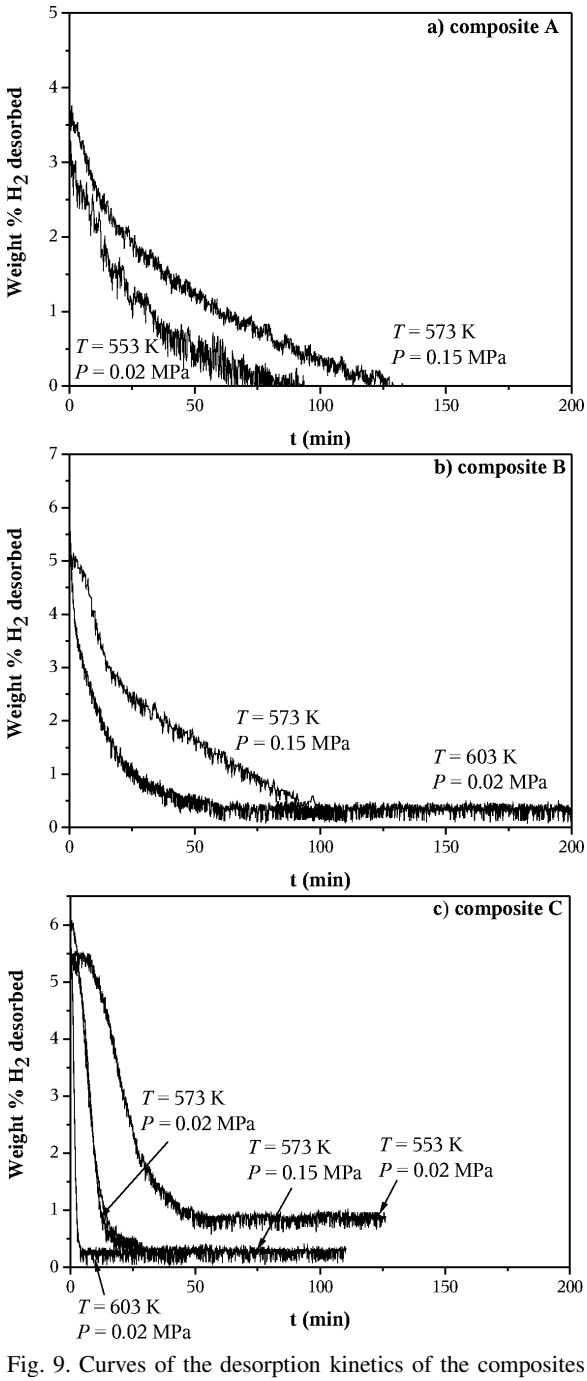


Fig. 9. Curves of the desorption kinetics of the composites at different temperatures and pressures: (a) composite A; (b) composite B; (c) composite C.

curves presenting the $d\alpha/dt = f(\alpha)$ dependence ($\alpha$ = conversion degree, Fig. 8) shows diffusion to become the rate controlling step first with sample A. With sample C the surface reaction continues to be rate limiting up to a higher $\alpha$ value. Since the surface reaction comprises dissociative chemisorption of hydrogen and nucleation, it is natural that the composite with the largest interface is the last one for which the transition from one rate-controlling step (surface reaction) to the other (diffusion) sets in. On the contrary, sample A is the first to be affected by hydriding limitation on behalf of the diffusion due to the lowest dispersion of this system, which also determines the more unfavorable absorption-desorption characteristics in this case.

The desorption of hydrogen from the composites under consideration is presented in Fig. 9. Dehydriding proceeds at $T$ = 553, 573 and 603 K and $P$ = 0.02 MPa as well as at $T$ = 573 K and $P$ = 0.15 MPa. The shapes of these curves show the best desorption kinetics for composite C at the temperatures and pressures used. This is probably due to the highest dispersion of this composite as mentioned above. With composites containing magnesium hydride, sample B is the one showing a more rapid desorption at 573 K and 0.15 MPa.

## Conclusion

The experimental results obtained on the absorption-desorption characteristics of composites containing the intermetallic compound 10 wt. % $Mg_2Ni_{0.8}Co_{0.2}$ in addition to $MgH_2$ or Mg illustrate the favorable catalytic effect of the $Mg_2Ni_{0.8}Co_{0.2}$ additive on these reactions. The hydriding kinetics of magnesium are improved significantly in all the systems investigated, the high absorption capacity being preserved even at temperatures below 573 K. With composites based on magnesium hydride the prolonged mechanical activation leads to an acceleration of the hydriding-dehydriding reactions and to higher absorption capacities at all temperatures within the range 573 – 373 K. It has been established that the results obtained with the composite 90 wt. % $MgH_2$-10 wt. % $Mg_2Ni_{0.8}Co_{0.2}$ activated mechanically for 180 min (B) are comparable with those for 90 wt. % Mg-10 wt. % $Mg_2Ni_{0.8}Co_{0.2}$ (C) activated mechanically for 30 min.

*Acknowledgement*

The present work was performed within the framework of the project INTAS No 05-1000005-7669.

[1] C. M. Stander, *Z. Phys. Chem*. **1977**, *104*, 229 – 238.
[2] C. M. Stander, *J. Inorg. Nucl. Chem*. **1977**, *39*, 221 – 223.
[3] J. Huot, G. Liang, S. Boily, A. Van Neste, R. Schulz, *J. Alloys Compd*. **1999**, *293 – 295*, 495 – 500.
[4] A. Zaluska, L. Zaluski, J. O. Ström-Olsen, *J. Alloys Compd*. **1999**, *289*, 197 – 206.
[5] J. Huot, G. Liang, R. Schulz, *Appl. Phys. A* **2001**, *72*, 187 – 195.
[6] M. Khrussanova, E. Grigorova, I. Mitov, D. Radev, P. Peshev, *J. Alloys Compd*. **2001**, *327*, 230 – 234.
[7] M. Khrussanova, M. Terzieva, P. Peshev, I. Konstanchuk, E. Ivanov, *Z. Phys. Chem*. **1989**, *164*, 1261 – 1266.
[8] M. Khrussanova, J.-L. Bobet, M. Terzieva, B. Chevalier, D. Radev, P. Peshev, B. Darriet, *J. Alloys Compd*. **2000**, *307*, 283 – 289.
[9] G. Liang, J. Huot, S. Boily, A. Van Neste, R. Schulz, *J. Alloys Compd*. **1999**, *291*, 295 – 299.
[10] Z. Dehouche, R. Djaozandry, J. Huot, S. Boily, J. Goyette, T. K. Bose, R. Schulz, *J. Alloys Compd*. **2000**, *305*, 264 – 271.
[11] Z. Dehouche, J. Goyette, T. K. Bose, R. Schulz, *Int. J. Hydrogen Energy* **2003**, *28*, 983 – 988.
[12] Z. Dehouche, T. Klassen, W. Oelerich, J. Goyette, T. K. Bose, R. Schulz, *J. Alloys Compd*. **2002**, *347*, 319 – 323.
[13] H. Gu, Y. Zhu, L. Li, *J. Alloys Compd*. **2006**, *424*, 382 – 387.
[14] E. Grigorova, M. Khristov, M. Khrussanova, J.-L. Bobet, P. Peshev, *Int. J. Hydrogen Energy* **2005**, *30*, 1099 – 1105.
[15] B. Tanguy, J.-L. Sonbeyroux, M. Pezat, J. Portier, P. Hagenmuller, *Mater. Res. Bull*. **1976**, *11*, 1441 – 1448.
[16] Z. Dehouche, T. Klassen, W. Oelerich, J. Goyette, T. K. Bose, R. Schulz, *J. Alloys Compd*. **2002**, *347*, 319 – 323.
[17] G. Barkhordarian, T. Klassen, R. Bormann, *J. Alloys Compd*. **2006**, *407*, 249 – 255.
[18] G. Liang, J. Huot, S. Boily, A. Van Neste, R. Schulz, *J. Alloys Compd*. **2000**, *297*, 261 – 265.
[19] M. Y. Song, J.-L. Bobet, B. Darriet, *J. Alloys Compd*. **2002**, *340*, 256 – 262.